



Study On Interface Fracture And Cohesive Constitutive Relation Of FRP Reinforced Concrete Structure

Felix Pinkrah Boafo, Professor Zhang Xuming

Abstract— With the constant deteriorating of concrete structures and high cost of reconstruction, the need to strengthen them as they age is very important. One of the ways is the use of Fiber Reinforced Polymers (FRP). For the past two decades, research into the use of FRP to strengthen existing concrete structures is on the rise with the bond between FRP and concrete of high importance.

With the evolution of these research fields, time is of the essence in this engineering world hence a valid finite elemental model will be of immense contribution. This current research seeks to analytically analyze the bond shear strength between FRP and concrete using ANSYS software. A control model is initially developed and compared with experimental and theoretical data developed by J. Yao et al. and, J.G. Teng and J.F. Chen respectively. The near-end supported (NES) single-shear pull test method was used.

Keywords— FRP, CFRP, Concrete, Ansys, Shear strength

I. INTRODUCTION

According to standards, the lifespan of reinforced structures are supposed to be between fifty (50) and one hundred (100) years[1]. Most of these structures starts deteriorating before the expected time and hence the need to repair them cannot be overlooked. Shear and flexural deficiencies exists in reinforced concrete structures with shear deficiencies being more dangerous. This is for the reason that failures due to shear deficiencies occur rapidly without distribution of internal forces[2]. Though these structures fail to meet strength standards and pose as a threat due to high chances of failure demolishing and reconstruction is usually not an option. Due to this the reinforcement market has grown greatly. The American society of civil engineers estimated in 2009 that about 2.2 trillion USD will have to be invested to bring the national infrastructure of the United States into a good condition[3].

FRPs are employed for concrete strengthening both as an internal component and external. However, externally bonded FRP has gained massive interest in the research world for some

decades now.

Globally, use of FRPs to strengthen concrete structures is a techniques that keeps drawing interest to itself[4]. Compared to steel plates, the easy mode of application, excellent corrosion resistance, high strength-to-weight ratio, non-magnetic properties, malleability, low creep, ease of construction, and superior durability led to the use of FRP instead of steel. Also, FRP bars have a lower modulus of elasticity compared to steel[5]. It has been proven both experimentally and theoretically that highly desired properties of a structure such as load carrying capacity, stiffness, ductility, performance under cyclic and fatigue loading and also environmental durability can all be increased by strengthening with FRP composites.

This article presents a finite element study on the bond shear strength between FRP and concrete using an NES single-shear pull test. The developed model is compared to experimental work done by Yao et al. and also theoretical calculations by Chen and Teng.

A. FRP Composite

FRP composites consists of long and continuous fibers (e.g. glass, carbon, etc.) bonded together with a resin matrix. The fibers provide the composites with their unique structural properties. The resin serves as the bonding agent to protect the fibers and to distribute the load among them. The earliest developer of FRPs used glass fibers inserted in polymeric resins that was provided by a company known as burgeoning petrochemical industries as early as the World War II[6]. As development of the composite world grew different fibers were discovered and used. Most commonly fibers used now are carbon, glass, aramid, and basalt with glass fibers being the most commonly used among them. Fig.1 shows the components of a composite on a stress and strain scale.

B. Failure Modes

In general, there exist about six different failure modes associated with FRP to concrete bonds. These are;

- Delamination of the FRP
- Adhesive failure
- Plate to adhesive interfacial failure
- Concrete to adhesive interfacial failure
- Plate tensile failure
- Concrete failure

This Research work is funded by The National Natural Science Fund

Felix Pinkrah Boafo: Hohai University, fpboafo@yahoo.com, No.1 Xikang Road Nanjing, PR China, 008613813944743

Professor Zhang Xuming: Hohai University, 19840038@hu.edu.cn, No.1 Xikang Road Nanjing, PR China, 008613813944743

However studies have showed that failure mainly occurs in the concrete for an FRP-Concrete bond subjected to shear. The failure are usually few millimeters away from the adhesive layer. Fig.2 is a schematic diagram of a typical pull test as described by Lu et al.[7]. The dotted line represents a fracture plane during a typical debonding failure with the fracture with being wider than the FRP.

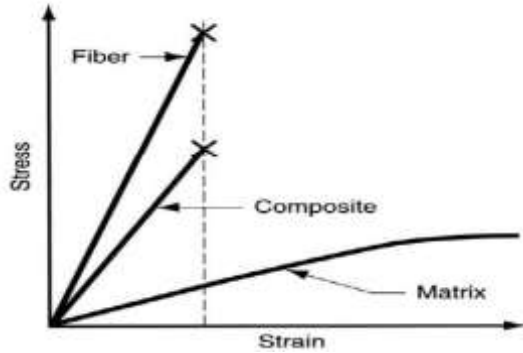


FIG.1. STRESS- STRAIN DIAGRAM FOR COMPOSITE PHASES

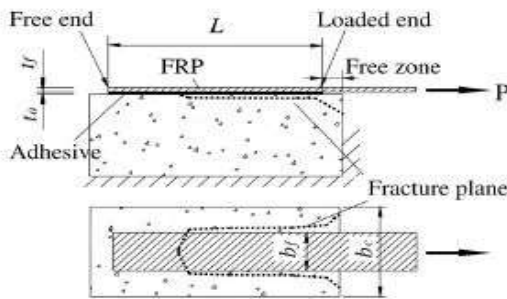


FIG.2. SCHEMATIC DIAGRAM OF A TYPICAL PULL TEST AS DESCRIBED BY LU ET AL.[7]

II. EXPERIMENT

Since the design and set up of the finite element model was based on the experiment made by Yao et al [1], it is necessary to describe briefly the setup used. In all about 72 specimens in seven different series were prepared. The concrete cube with a dimension of $150 \times 150 \times 350$ was used for five series (I, II, IV, VI, and VII). A dimension of $100 \times 150 \times 350$ was used for the remaining two series (III and V). Material properties of the cubes were determined by the BS 1881 [8].

For the FRP component of the test, two types were used. GFRP and CFRP. GFRP was used for the III-7 and III- 8 test samples while CFRP was used for the rest. The tensile strength of the FRPs were determined using the ASTM D3039/ D3039M-95a[8]. The mechanical properties of the FRP used are as stated in Table I.

Table I

FRP type	Thickness (mm)	Tensile strength f_{frp} (MPa)	Elastic modulus E_{frp} (GPa)	Ultimate tensile strength ϵ_{frp} (%)
GFRP	1.27	351	22.5	1.56
CFRP	0.165	4114	256	1.61

A. Test Setup

Fig.3 represent a schematic diagram of the test setup as used by Yao et al [9]. The setup involved a special fabricated steel rig for the test.

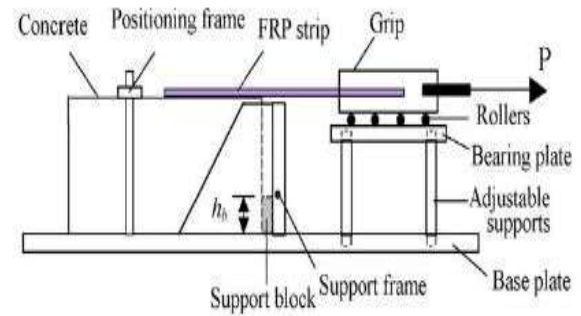


Fig.3. Schematic Diagram of Test Setup

III. NUMERICAL MODEL

Another standard for the verification of the finite element result is the Cheng and Teng model. This makes it appropriate to give an overview of this model. The Chen and Teng model was focused on addressing some shortcoming of previous models[10]. The target was to design a new model that was simple, practical, logically based and has the capabilities of capturing the fundamental features of the FRP to concrete bond behavior and as well be as accurate as possible in predicting the bond strength and effective bond length. Chen and Teng after studying various numerical models such as Holzenkampfer's model and the Wu et al.'s model[11] noticed some shortcomings and hence developed a new model. The new model developed was intended to be used "for practical design that is simple to use, rationally based, and capable of capturing the fundamental features of the bond behavior and predicting the bond strength and the effective bond length with good accuracy"[12].

In the model the bond strength P_u was defined as,

$$P_u = 0.427\beta_p\beta_L\sqrt{f'_c b_p L_e} \quad (1)$$

With the width ration effect, β_p , defined as

$$\beta_p = \sqrt{\frac{2 - b_p/b_c}{1 + b_p/b_c}} \quad (2)$$

$$\beta_L = \begin{cases} 1 & \text{if } L \geq L_e \\ \sin \frac{\pi L}{2L_e} & \text{if } L < L_e \end{cases} \quad (3)$$

$$L_e = \sqrt{\frac{E_p t_p}{\sqrt{f'_c}}} \quad (4)$$

β_p refers to the width of the FRP plate in mm, β_p and β_L are dimensionless coefficients establishing the effects of the FRP-to-concrete width ratio, L_e is the effective bond length in mm and f'_c is the cylinder compressive strength of concrete in MPa. Cheng and Teng[12] reduced the coefficient value in equation one to 95% of the initial value for purposes of designing the ultimate strength.

IV. ANSYS MODEL

In this paper, the goal was to develop a finite element (FE) model to simulate the NES test and compare the results with existing data. The ANSYS finite element analysis software (ANSYS 14.5) was used for all finite element modeling. The model was created in a 3-dimensional plane to represent the concrete and FRP.

Two different elements were used in the model. SOLID 65 was the element used for the concrete modeling. SOLID 65 is used for the three-dimensional modeling of solids with or without reinforcing bars (rebars). It has the capabilities of cracking in tension and crushing in compression. SHELL 41 elements were used to model the FRP. SHELL 41 is a 3-D element having membrane (in-plane) stiffness but no bending (out-of-plane) stiffness. It is intended for shell structures where bending of the elements is of secondary importance.

A. Material Properties

For the modeling of the NES test consist of two material models. Material model 1 represented the concrete. The concrete modulus of elasticity (EX) was established from equation (5) and a Poisson's ratio (PRXY) of 0.2 was used. The material model 2 represented the FRP with an elastic modulus of 256 GPa and a Poisson's ratio of 0.3.

To define the failure of the concrete, the multilinear isotropic material uses the Von Mises failure criterion together with the Willam and Warnke model[13]. The stress and strain values were established for the concrete.

$$E_c = 4700\sqrt{f'_c} \quad (5)$$

$$f = \frac{E_c \times \varepsilon}{1 + \left(\frac{\varepsilon}{\varepsilon_o}\right)^2} \quad (6)$$

$$\varepsilon_o = \frac{2f'_c}{E_c} \quad (7)$$

f'_c is the cylinder compressive strength of the concrete, ε is the strain at stress f , ε_o strain at the ultimate compressive stress f'_c .

B. Modeling

A rectangular coordinate system was created at the active working plane. Four solid blocks were generated and glued together. The glued volume represented the concrete substrate. The substrate was broken down to four volumes to enable easy modeling of the CFRP.

Table II. Results Comparison

Sample	Concrete cylinder strength (Mpa)	FRP width (mm)	FRP bond length (F_{frp}) (mm)	Test Failure Load (TFL) (KN)
IV-2	18.9	25	95	5.90

created nodes with the concrete substrate. This was done based on assumption that there existed a perfect bond between the FRP and concrete. For the validation of the model, the dimensions used for both the FRP and concrete were as the dimensions of the concrete used in the experiment.

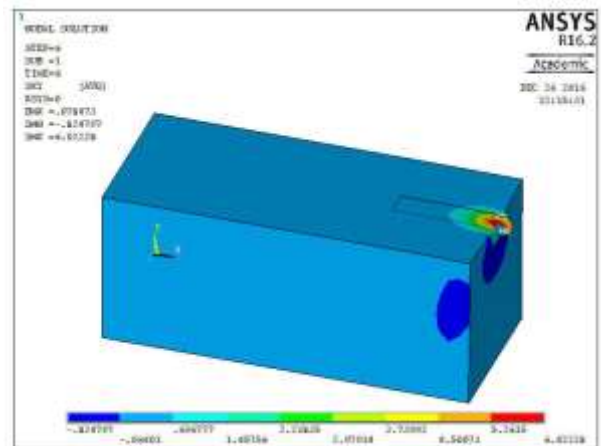


Fig.4. XY-Shear Stress Deformation

C. Model Validation

The ANSYS model was validated by comparing the XY shear stress failure values to experimental work done by Yao et al.[9] and predicted results from the Cheng and Teng model[12]. The ANSYS results showed a very close correlation to that from the experiment and predicted values. Table II shows values from ANSYS as compared to both experimental and predicted.

V. PARAMETRIC ANALYSIS

A. FRP Thickness Effect

Previous research indicates that the variation of the FRP thickness has an effect on the bond strength between FRP and concrete. In order to prove this theorem with the NES single-shear test, five different thicknesses of FRP were investigated to ascertain its effects on the shear strength between the FRP and concrete.

As expected, the maximum shear stress at failure of the test sample increases with an increase in the thickness of the FRP for the same applied load. This finding is confirmed by a study done by Maalej and Leong in 2005[16]. Their study showed that with an increase in the thickness of the FRP there was also an increase in the interfacial shear stress concentration.

Fig. 5 represents a graph of the concrete's Von Mises stress against the corresponding shear stress. As the applied load increased both parameters also increased until failure of the concrete beam. Focus was placed on the failure of the concrete since as a rule of thumb, for any composite material the system is taken as failed when one of the components fails.

Fig. 6 gives a graphical representation of the thickness of the FRP as compared to the shear stress value at failure. From Figure 6 it can be seen that with an increase of the FRP thickness from 0.165mm to 0.2mm, which is about 21.2% increase, saw an increase of the shear stress at failure from 5.73 to 6.46 which constitutes an increase of 12.78%. Also an increase from 0.2mm to 0.4 mm (100% increase) led to only 14.65% the failure shear strength. Another 100% increase in the thickness of the FRP (0.4mm to 0.8mm) led to an increase of about 10.66% in the shear stress recorded at failure.

A further increase of the thickness from 0.8mm to 1.6mm only saw an increase in the shear stress at failure by 4.27%. It can be noticed that as the FRP thickness increased there was an increase in the corresponding failure shear stress but there was a decrease in the percentage increase in the shear stress.

Table III. FRP Thickness Variations

Sample	FRP Thickness (mm)
TH-1	0.2
TH-2	0.4
TH-3	0.6
TH-4	0.8
TH-5	1.0

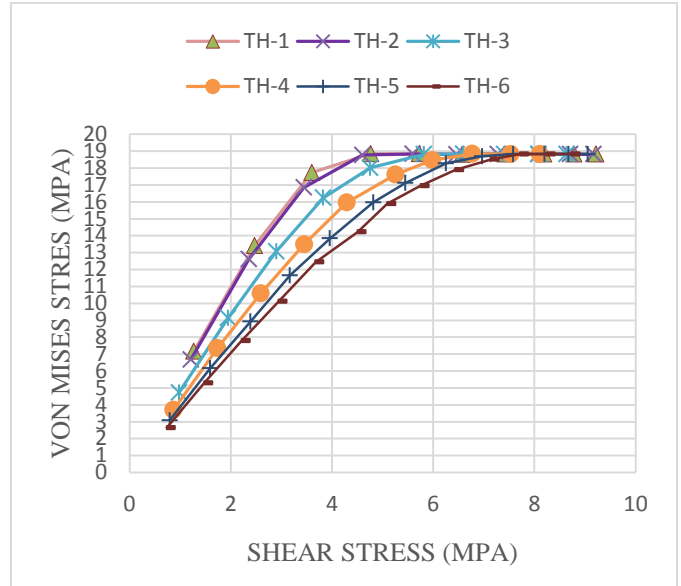


Fig.5. A graph of concrete Von misses stress against the shear stress

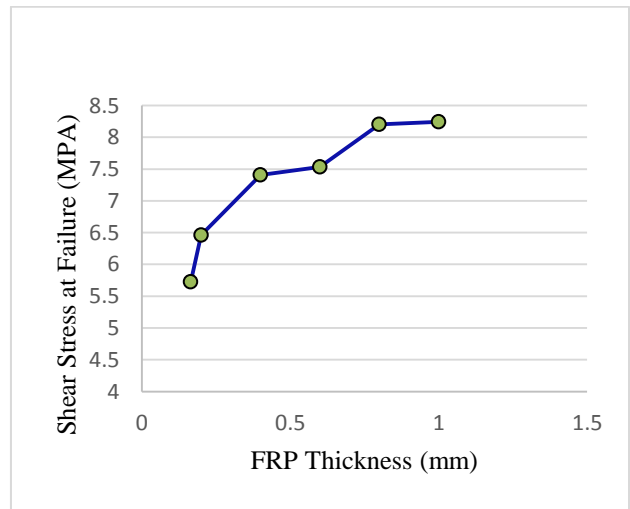


Fig.6. A graph of concrete Von misses stress against the shear stress at failure

B. FRP Young Modulus

The young modulus of the FRP used depends on the various young modulus of the individual component. The young modulus of FRPs varies. For a typical carbon FRP (CFRP), the young modulus varies from 160 GPa to values as high as 540 GPa[9]. For glass FRPs the young modulus ranges between 70 GPa and 90 GPa. The values examined are as listed in Table IV.

The effects of the young modulus on the shear stress are as presented in Fig.7. The shear stress value at failure of the reinforced concrete increased with increase in the young modulus. The first trail value was as low as 50 GPa. At this value the shear stress attained at failure was only 4.97709. Increasing the young modulus t 100 GPa (100% increase) only saw the shear stress value increasing to just about

5.11821 which is just about 3% increase in the shear stress. A further look at a young modulus value of 200 GPA which is another 100 % increase from 100 GPA also saw an increase in the shear stress at failure. The shear stress increase at a percentage of about 14.2%. At 300 GPA the shear stress at failure was 6.4729. The difference in the shear stress attained at 50 GPA and the attained at 300 GPA is about 1.49581 which amounts to about 30% increase thought the young modulus of the material was increase by 500%.

Table IV. FRP Young Modulus Parameters

Sample	Young Modulus (GPA)
YM-1	50
YM-2	100
YM-3	200
YM-4	256
YM-5	300

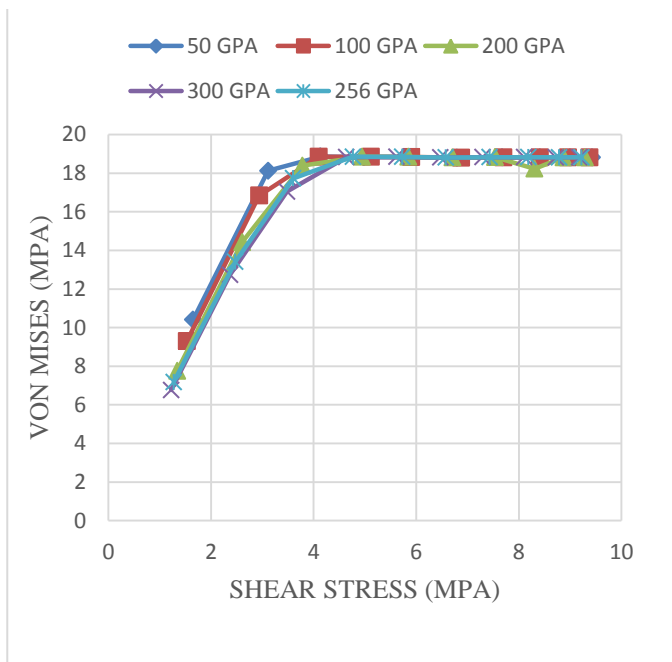


Fig.7. A graph of concrete Von misses stress against the shear stress with Varying FRP Young Modulus

It is clear that an increase in the stiffness of the FRP material does influence the shear capacity of the entire structure but the effect compared to the value increase in shear stress is not that high.

C. Concrete Young Modulus Effect

As already establish and is true for every composite material, the structure fails when one of these fail. In a concrete and FRP bond, the concrete is the weaker component, when it fails the entire strengthening fail. Since

most of the failures associated with FRP strengthened concrete occurs in the concrete beam a study was carried out to analyze the effect of the concrete's young modulus on the entire structure. Five (5) different cylinder compressive strength of concrete were examined and the shear stress of the strengthened component at failure was observed and also the percentage of the young modulus that was utilized till failure.

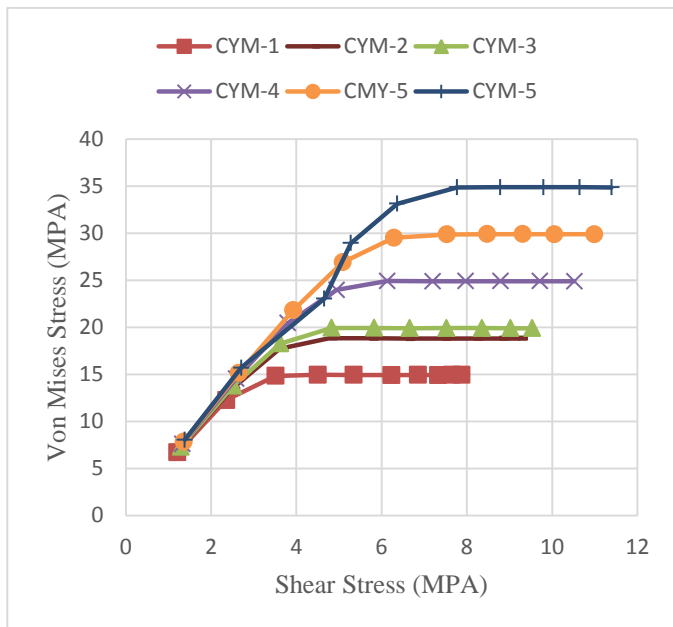
Table V. Concrete Cylinder Compressive Strength

Sample	Cylinder Compressive Strength (MPa)
CYM-1	15
CYM-2	18.9
CYM-3	20
CYM-4	25
CYM-5	30
CYM-6	35

Table VI represents the various failure loads with their corresponding shear stresses and Von Mises stress values at failure. A quick glance at the table shows that as the cylinder compressive strength of the concrete increases, the shear stress at failure also increases. Though for samples CYM-1, CYM-2 and CYM-3 the applied load did not increase there was an increase in the shear stress. Also the percentage of the cylinder compressive strength utilized at failure increased. It can be concluded that though the applied load is the same the required time for failure increases as the cylinder compressive strength also increases. This means a long structural life. Also comparing sample CYM-5 and CYM-6, the failure load stayed the same but there was an increase of 5.23% and the compressive strength utilized at failure also increased by 0.03%.

The increase in the shear stress with increase in the concrete cylinder compressive strength can be attributed to the increase in stiffness of the concrete. With the increase in the concrete cylinder compressive strength, there comes a corresponding increase in the elastic modulus of the concrete. Since stiffness is directly proportional to the young modulus, its increase leads to the increase of stiffness. This leads to a higher resistance of deformation and hence reducing the rate of failure of the component.

Fig.8 represents a graphical representation of the Von Mises stress against the shear stress of the various samples.



VI. CONCLUSION

In this paper, the NES shear strength test was modeled using Ansys software. The results generated was validated with existing experimental and theoretical values and proven to be correct.

The parametric study showed that

- An increase FRP thickness increases the shear strength of the component
- The young modulus of both FRP and concrete affects the shear strength of the component.

ACKNOWLEDGMENT

The authors are grateful for the financial support from Hohai University (G-V784) and from the Research Grants Council.

REFERENCES

- [1] "EN 1992-1-1 (2004) (English): Eurocode 2: Design of concrete structures - Part 1-1: General rules and rules for buildings," vol. 1, 2011.
- [2] A. Belarbi, S. W. Bae, and A. Brancaccio, "Behavior of full-scale RC T-beams strengthened in shear with externally bonded FRP sheets," *Constr. Build. Mater.*, vol. 32, pp. 27–40, 2012.
- [3] A. S. of C. Engineers, 2009 REPORT CARD FOR AMERICA'S INFRASTRUCTURE ADVISORY COUNCIL. 2009.
- [4] L. Teng J. G. , Chen, J. F. ,Smith, S.T., Lam, "FRP-Strengthened RC Structures," John Wiley Sons, Ltd., 2002.
- [5] C. Dundar, A. Kamil, and R. J. Frosch, "Prediction of load – deflection behavior of multi-span FRP and steel reinforced concrete beams," *Compos. Struct.*, vol. 132, pp. 680–693, 2015.

- [6] V. L. Brown and J. J. Lesko, "FRP composites for construction : State-of-the- art review Fiber-Reinforced Polymer Composites for Construction — State-of-the-Art Review," no. May 2016.
- [7] X. Z. Lu, J. G. Teng, L. P. Ye, and J. J. Jiang, "Bond-slip models for FRP sheets/plates bonded to concrete," *Eng. Struct.*, vol. 27, no. 6, pp. 920–937, 2005.
- [8] "Astm D3039/D3039m-95a. Standard test method for tensile properties of polymer matrix composite materials," 1995.
- [9] J. Yao, J. G. Teng, and J. F. Chen, "Experimental study on FRP-to-concrete bonded joints," *Compos. Part B Eng.*, vol. 36, no. 2, pp. 99–113, 2005.
- [10] Z. S. Hiroyuki, Y. , Wu, "Analysis of debonding fracture properties of CFS strengthened member subject to tension," pp. 287–294, 1997.
- [11] H. Wu, Z., Yuan, H., and Niu, "Experimental/Analytical Study on Interfacial Fracture Energy and Fracture Propagation Along FRPConcrete Interface," *Fract. Mech. Concr. Mater.*, vol. 201, pp. 133–152, 2001.
- [12] T. G. Chen, J. F., "ANCHORAGE STRENGTH MODELS FOR FRP AND STEEL PLATES," no. c, pp. 784–791, 2001.
- [13] K. Willam and E. Warnke, "Constitutive model for the triaxial behavior of concrete," *Int. Assoc. Bridg.*, pp. 1–30, 1975.
- [14] J. K. Macgregor, James G. Wight, DESIGN, REINFORCE CONCRETE MECHANICS & Design. 2009.
- [15] R. Santhakumar and E. Chandrasekaran, "Analysis of Retrofitted Reinforced Concrete Shear Beams using Carbon Fiber Composites," vol. 4, 2004.
- [16] M. Maalej and K. S. Leong, "Effect of beam size and FRP thickness on interfacial shear stress concentration and failure mode of FRP-strengthened beams," *Compos. Sci. Technol.*, vol. 65, no. 7–8, pp. 1148–1158, 2005. University Science, 1989.